

ALL-DIELECTRIC FREQUENCY SELECTIVE SURFACES WITH FEW NUMBER OF PERIODS

J. H. Barton¹, R. C. Rumpf^{1,*}, R. W. Smith¹, C. Kozikowski², and P. Zellner²

¹EM Lab, W. M. Keck Center for 3D Innovation, University of Texas at El Paso, USA

²Prime Photonics LC, Blacksburg, VA 24060, USA

Abstract—All-dielectric frequency selective surfaces (FSSs) can serve as an alternative to their metallic counterparts when they must operate at very high power, loss must be minimized, or when the surface itself must be low observable. When metals are avoided, there is a weaker interaction with electromagnetic waves and it becomes more difficult to achieve strong suppression in the stop band while also realizing compact size, wide field-of-view or broadband operation. One attractive approach utilizes guided-mode resonance (GMR) as the filtering mechanism, but this phenomenon exhibits several drawbacks that must be overcome for practical application at radio frequencies. This paper introduces the concept of guide-mode resonance for FSSs and describes how they can be made to operate with a dramatically fewer number of periods than conventional GMR devices.

1. INTRODUCTION

Frequency selective surfaces (FSSs) are planar structures composed of a periodic array of elements that filter electromagnetic waves incident on the surface [1–3]. They are most well-known for their applications in stealth technology [4] and modification of radar cross section [5], but many other applications exist including the construction of radomes [6–8], dichroic sub-reflectors [9], lenses [10], radio frequency identification (RFID) [11], and protection from electromagnetic interference.

Conventional FSSs are constructed from metallic screens or dipole arrays to exploit the strong interactions between electromagnetic waves and metals [12]. Metals are problematic, however, at very high power,

Received 24 April 2012, Accepted 1 June 2012, Scheduled 11 June 2012

* Corresponding author: Raymond C. Rumpf (rcrumpf@utep.edu).

when losses must be absolutely minimized, or when the device itself must be low observable [13]. The problem of arching at high power is particularly severe with metal FSSs, so all-dielectric structures are an attractive alternative because the field can be distributed over larger area. Currently, all-dielectric FSSs are a highly immature technology and exhibit a number of drawbacks that have, so far, limited their widespread use at radio frequencies. This paper addresses the size of all-dielectric FSSs and presents a novel solution for miniaturizing them using guided-mode resonance (GMR).

GMR filters are the combination of two simple devices; a grating and a slab waveguide that are electromagnetically coupled [14–16]. This simple combination makes the device highly compact and easy to build. When precise phase matching conditions are met, an external wave incident on the device is diffracted by the grating and partially coupled into guided modes within the slab. As long as the guided modes overlap the grating, they slowly leak from the slab over some distance due to reciprocity. The outcoupled wave interferes with the applied wave to produce an overall frequency response. GMR filters can produce very strong suppression using just a single subwavelength dielectric layer and low dielectric contrast.

GMR filters are almost always designed assuming that the grating is infinitely periodic. Due to the physics of guided mode resonance, devices must often be hundreds of grating periods long for a finite-size structure to approach the performance of the infinitely periodic structure [17]. At radio frequencies, this often leads to prohibitively large devices that are dozens of meters in length.

This work describes a procedure to overcome this size limitation. It was used to design a simple narrow band GMR filter operating at 1.5 GHz that would normally require over 200 grating periods to operate. The device was designed to operate at normal incidence and with the electric field polarized parallel to the grating grooves. Using the technique described in this paper, the GMR filter provided strong suppression in the stop band using just seven grating periods. This represents nearly $30\times$ reduction in size. It is important to note that the device presented here is narrow band and has a narrow FOV. The bandwidth and FOV can be dramatically extended through more sophisticated grating designs [18], but these topics will not be discussed here.

2. GUIDED-MODE RESONANCE FILTERS

GMR filters are formed whenever a slab waveguide and a grating are brought into close proximity so that they are electromagnetically

coupled. They are simple structures that are highly compact, easy to manufacture, and can be monolithic; made from the same low loss dielectric. The bandwidth of the device can be made arbitrarily small by reducing the contrast of the grating. The filter response can be made symmetric with virtually no ripple outside of the pass band for both transmission and reflection type filters. Efficiency can approach 100% on resonance and devices can be constructed with multiple resonances.

There are two physical mechanisms occurring simultaneously and each must be understood to fully explain guided mode resonance. The first is diffraction from a grating and is illustrated in Figure 1.

The amplitudes of the diffracted modes are found by solving Maxwell's equations, but the directions are quantified through the famous grating equation [19, 20].

$$\sqrt{\varepsilon_{\text{avg}}} \sin \theta_m = \sqrt{\varepsilon_{\text{inc}}} \sin \theta_{\text{inc}} - m \frac{\lambda_0}{\Lambda} \tag{1}$$

In this equation, ε_{avg} is the average dielectric constant where the direction of the modes are being calculated, ε_{inc} is the dielectric constant outside the GMR filter, θ_m is the angle of the m th diffracted mode, θ_{inc} is the angle of incidence of the applied wave, λ_0 is the free space wavelength, and Λ is the period of the grating. Gratings with periods longer relative to the wavelength will diffract into more modes. The angles of the diffracted modes depend on the diffraction order, materials, wavelength, and grating period and are calculated from the grating equation.

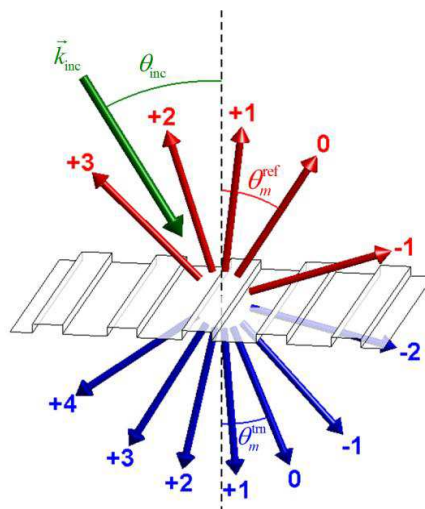


Figure 1. A grating diffracts an applied wave into discrete modes.

The second mechanism is guiding within the slab. Wave guiding can only occur when the effective dielectric constant of the guided mode is greater than the surrounding media and less than the dielectric constant of the slab itself. This condition can be quantified as

$$\sqrt{\varepsilon_{\text{inc}}} \leq \left| \frac{\beta_m}{k_0} \right| < \sqrt{\varepsilon_{\text{avg}}} \quad (2)$$

where k_0 is the free space wave number, and β_m is the propagation constant of the m th order mode. From the ray-tracing view of a slab waveguide, a guided mode can be envisioned as a ray propagating at an angle θ_m within the slab. This is related to the propagation constant through

$$\frac{\beta_m}{k_0} = \sqrt{\varepsilon_{\text{avg}}} \sin \theta_m \quad (3)$$

Guided-mode resonance occurs only when the angle of the diffracted mode matches exactly that of a guided mode in the slab. At resonance, the propagation constant can be related to the angle of incidence by substituting Eq. (3) into Eq. (1). A condition for guided-mode resonance is derived by combining this with Eq. (2).

$$\sqrt{\varepsilon_{\text{inc}}} \leq \left| \sqrt{\varepsilon_{\text{inc}}} \sin \theta_{\text{inc}} - m \frac{\lambda_0}{\Lambda} \right| < \sqrt{\varepsilon_{\text{avg}}} \quad (4)$$

Equation (4) can be used to identify the regions of resonance as a function of angle of incidence and grating period. A diagram was generated for the GMR filter described in this paper and is shown in Figure 2.

Some important attributes of GMR filters can be observed in this diagram. First, the positions of the resonances are a function of the angle of incidence and grating period. Second, the number of resonances increases as the grating period is increased relative to the wavelength due to the existence of multiple diffracted modes.

With this background, the overall operation of the GMR filter can be understood. An applied wave is diffracted by the grating into a number of discrete modes. When a precise phase matching condition is satisfied, a diffracted mode exactly matches a guided mode supported by the slab waveguide and a resonance is excited over a narrow band of frequencies. At resonance, the applied wave is partially coupled into the guided-mode across the entire aperture of the FSS. The remaining energy is either reflected or transmitted through the FSS. The portion of energy coupled into the guided mode propagates through the slab waveguide, but slowly leaks from the slab due to the interaction with the grating. This leakage is a necessary condition to satisfy the reciprocity theorem [21]. Waves out-coupled on either

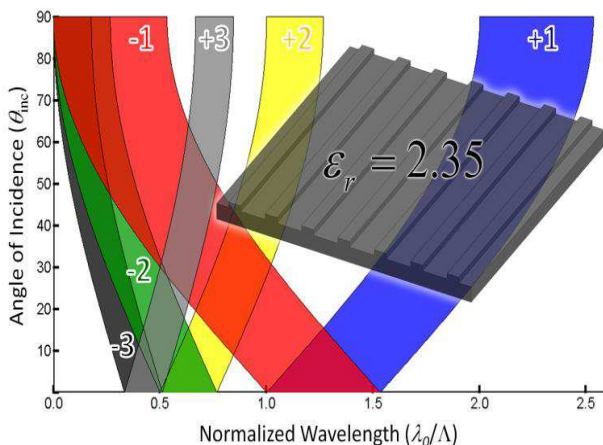


Figure 2. Regions of resonance for the GMR filter described in this paper.

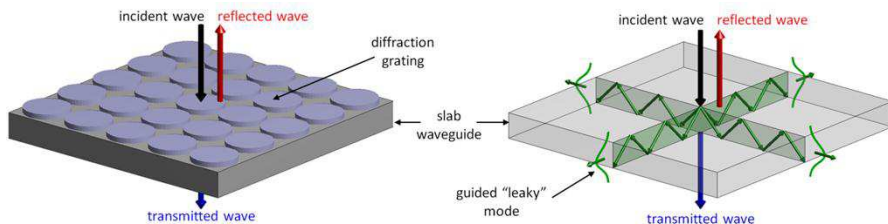


Figure 3. Illustration of physical mechanisms leading to guided-mode resonance.

side of the FSS combine out of phase with reflected and transmitted portions of the applied wave to produce an overall frequency response. The guided mode resonance concept is illustrated in Figure 3.

Outside of the FSS, the diagram shows the incident, reflected, and transmitted waves. Inside the slab, ray traced versions of the guided modes are shown.

3. BASELINE DESIGN

Work began by choosing a frequency and material system. A frequency of 1.5 GHz was chosen because it was a sufficiently low frequency to demonstrate the concept while keeping the physical dimensions of the device reasonable for easy manufacturing and handling in an anechoic chamber. High density polyethylene (HDPE) was chosen as

the dielectric material because it is inexpensive, easily machined, and has a low loss tangent. The dielectric constant was specified by the vender to be $2.35 \pm 10\%$. Despite this uncertainty, the design was performed using 2.35 as the dielectric constant.

Given the frequency and material system, a simple three step procedure was used to design a monolithic GMR filter. This was considered to be the baseline design because it was designed as an infinitely periodic device. The procedure is illustrated in Figure 4.

The first step was to design a two layer structure that provided a low background reflection across the band of interest. Here, each layer was assumed to be homogeneous. To eventually design a GMR filter that was to be monolithic, the dielectric constant in the top layer ϵ_1 was constrained to fall between the dielectric constant of the surrounding material (air) and the dielectric constant of the HDPE, $1.0 < \epsilon_1 < 2.35$. A transfer matrix method [22] was used to model transmission through the two layer dielectric stack. A least squares optimization method was then implemented in MATLAB to determine the values of ϵ_1 , d_1 , and d_2 that minimized the background reflection for a wave at normal incidence. These were found to be $\epsilon_1 = 1.1$, $d_1 = 1.999$ cm, $d_2 = 5.588$ cm.

The second step was to realize ϵ_1 in the top layer using a grating

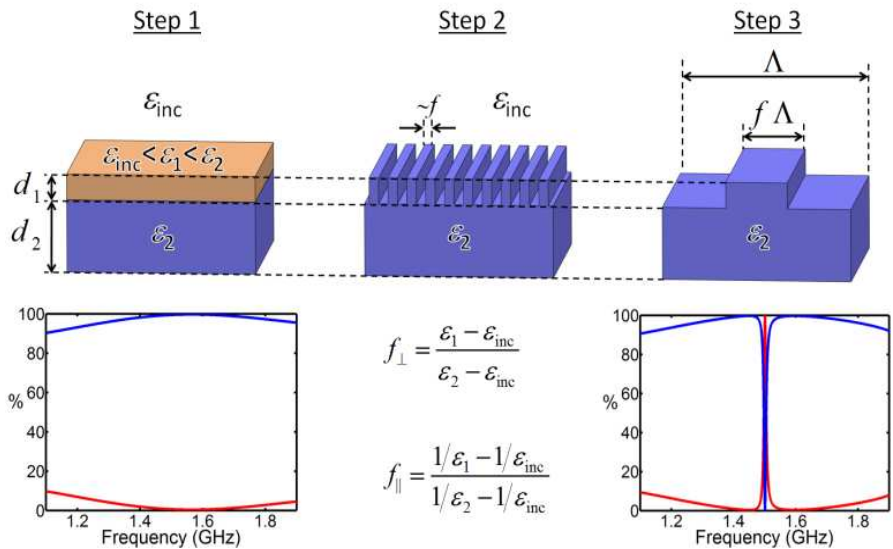


Figure 4. Three step design procedure for an infinitely periodic GMR filter.

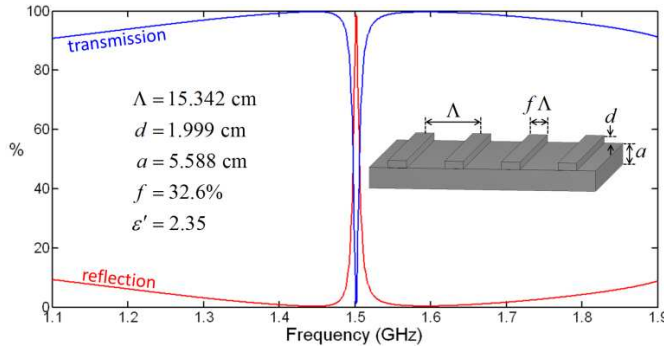


Figure 5. Baseline GMR design and its simulated performance.

with the correct duty cycle. This was accomplished using effective medium theory [23] that relates the duty cycle f of the grating to the effective dielectric constant for a normally incident wave. For one-dimensional gratings, two polarizations are possible so there are separate equations for calculating the duty cycle necessary to realize the needed effective dielectric constant. These are summarized in Eqs. (5) and (6). The design described here had the electric field polarized parallel to the grooves so Eq. (5) was used. f_{\perp} was calculated to be 32.6%.

$$\epsilon_1 = f_{\perp} \epsilon_2 + (1 - f_{\perp}) \epsilon_{\text{inc}} \tag{5}$$

$$\frac{1}{\epsilon_1} = \frac{f_{\parallel}}{\epsilon_2} + \frac{1 - f_{\parallel}}{\epsilon_{\text{inc}}} \tag{6}$$

The third step was to adjust the grating period until a guided-mode resonance was placed at the desired frequency. To aid in this step, an initial guess at the grating period can be taken from Figure 2 as $\Lambda = 0.8\lambda_0$. Rigorous coupled-wave analysis [24] was used to tune the grating period until the resonance fell exactly on 1.5 GHz. This was found to be $\Lambda = 15.34 \text{ cm}$. The final design, along with the simulated transmittance and reflectance, is provided in Figure 5.

4. EFFECT OF FINITE LENGTH

No physical device can be made infinitely periodic. Real devices must be constructed using only a finite number of grating periods. For low contrast GMR filters, it often takes hundreds of grating periods for a guided-mode to leak from the slab waveguide. Similarly, an applied wave must overlap hundreds of grating periods to excite a sufficiently strong guided-mode so as to produce a strong resonance condition.

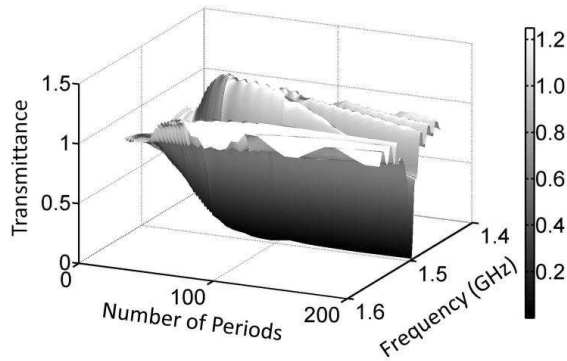


Figure 6. Response of a GMR filter with varying number of periods.

This means that for a real device to approach the performance of the infinitely periodic device, it must be composed of hundreds of grating periods [17].

To quantify this, a series of simulations was performed using the finite-difference frequency-domain (FDFD) method [25]. These simulations started with the baseline GMR and simulated finite length devices with an increasing number of grating periods. The results are provided in Figure 6. From this data, it can be observed that real devices will exhibit increased ripple with weakened and broadened resonance relative to the infinitely periodic device. For the baseline GMR, it can be concluded that at least 200 periods are needed for a sufficiently strong frequency response.

5. APPROACH

To date, almost all implementations of GMR filters have been at optical frequencies where accommodating a large number of grating periods is not a problem. At radio frequencies, however, this results in prohibitively large devices. Two hundred periods of the baseline GMR is over 30 m in length. Clearly, for practical implementation at radio frequencies a solution to this is needed. In fact, it was necessary to find a method capable of producing a strong frequency response using a GMR with just five to ten periods.

Some preliminary investigations focused on using anti-reflective terminations at the end of the slab. Ultimately this did not work because a sufficiently strong guided mode was never excited. This is a necessary condition that ensures the out-coupled waves have sufficient amplitude to completely interfere with the applied wave. The technique that was ultimately successful was terminating the

slab waveguide with reflective ends. With reflective ends, the device effectively “unfolds” into an infinitely periodic device. At the start, it was hypothesized that the round trip phase of the guided mode in the slab should be an integer multiple of 2π to prevent the mode from interfering with itself and scattering out of the slab. To match this condition to the designed resonant frequency, spacer regions were added to the ends of the slab that could be adjusted in length. The conceptual construction of the device is illustrated in Figure 7.

To study this device and produce a design, a double parameter sweep was performed showing transmittance as a function of frequency and spacer length. The results are shown in Figure 8. It was initially anticipated that the device response would be erratic when the spacers were not tuned to the resonant frequency of the baseline GMR. It was surprising to observe a reasonably strong resonance for all spacer lengths. This means that a device’s performance will be robust to errors incurred in the spacer length due to fabrication. The strongest suppression was observed at the point where the spacers were tuned to the same frequency as the baseline GMR confirming the original hypothesis, but the response away from these values was still very useful. Based on this analysis, the optimum length for the spacer regions was found to be 4.3 cm.

From the data in Figure 8, it was discovered that the position of

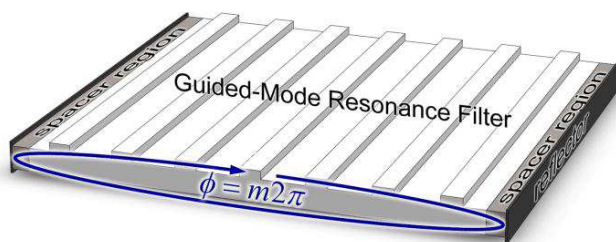


Figure 7. Construction and operational principle of a few-period GMR filter.

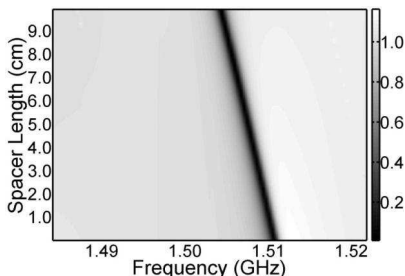


Figure 8. Double parameter sweep for a seven period GMR filter.

the resonance could actually be tuned through the length of the spacer regions. Devices with fewer periods provided the widest tuning range. Devices with more periods were less tunable and also exhibited multiple resonances corresponding to multiple resonant modes oscillating in the slab.

While not conveyed by this data, an approximately 3 dB improvement in suppression on resonance was observed for every grating period added to the GMR.

6. EXPERIMENTAL RESULTS

The final design of the device is shown in Figure 9. It had the same geometry as the baseline GMR, but included seven grating periods and two spacer regions on either end that were 4.3 cm in length.

Two support frames were crafted in order to orient the GMR in a position allowing a vertically polarized field pattern to be parallel to the grooves in the GMR. The first support frame consisted of two sides made of medium-density fibreboard (MDF) sandwiched between sheet metal siding. The sheet metal siding was employed as the reflector panels. The second support frame contained no metal side walls. The GMR was inserted inside the support frame and placed on a table inside an anechoic chamber 30 inches in front of the receiver antenna as displayed in Figure 10.

The measurement setup consisted of two linearly polarized 15 dB gain horn antennas that operated across the 1.2 to 1.7 GHz band. The transmitting horn antenna was connected to Port 1 of an Agilent 8720 Vector Network Analyzer (VNA) while the receiver horn antenna was connected to Port 2. The VNA was controlled via ORBIT software allowing the entire measurement to be computer controlled.

The anechoic chamber system was carefully calibrated prior to the

Table 1. Dimensional variations between the simulated design and the fabricated test structure.

PARAMETER COMPARISON		
Parameter	Designed	Measured
Λ	15.342 cm	15.400 cm
a	5.588 cm	5.398 cm
d	1.999 cm	1.905 cm
s	4.3 cm	4.207 cm
f	32.6%	32.99%

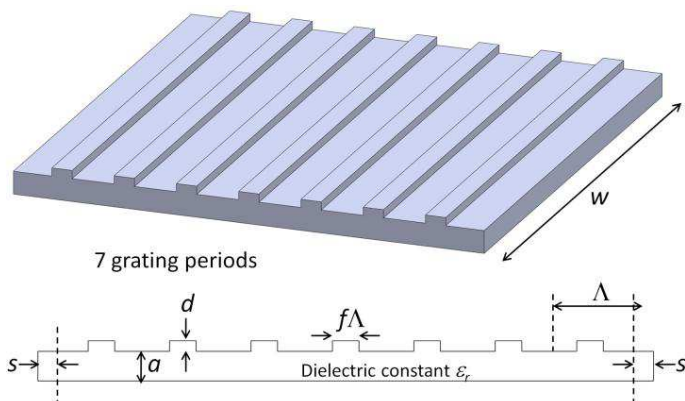


Figure 9. Final design of seven period GMR.



Figure 10. All-dielectric FSS with few periods setup inside an anechoic chamber.

insertion of the GMR in order to eliminate the effects of the table and the antenna support structures. The measurements were made over a frequency band of 1.4 to 1.6 GHz. The measured transmission results are provided in Figure 11 and Figure 12.

Figure 11 details the magnitude response of the GMR versus frequency while Figure 12 depicts the phase response of the GMR with respect to frequency, both with and without the metal walls.

As can be noted in the figures, when the metal walls were present, a strong resonance occurred at 1.491 GHz. However, when the metal walls were removed, no resonance was observed. This is very consistent with the simulated results discussed previously.

Figure 12 depicts the measured response along with the simulated response. From the figure it can be noted that the measured response shows a resonance at a slightly higher frequency in comparison to the simulated response. The frequency shift was attributed to fabrication

error. A comparison between the designed parameters and the actual fabricated parameters is depicted in Table 1.

After the FDFD model was modified with the measured dimensions, position of the resonance was accurately predicted, but the measured resonance was slightly broader than that of the simulated device. This was attributed to the loss tangent of the dielectric not being included in the simulation. By not including the loss tangent in this version of the FDFD code, the simulated response maintained a

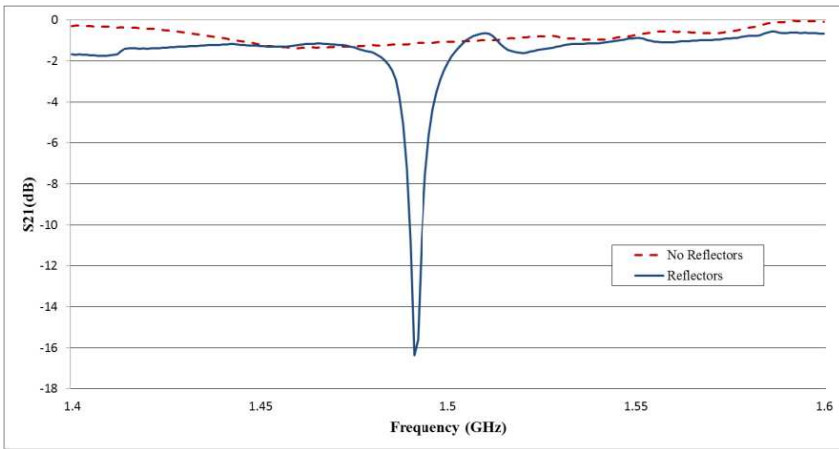


Figure 11. Measured transmittance vs. frequency with and without reflectors.

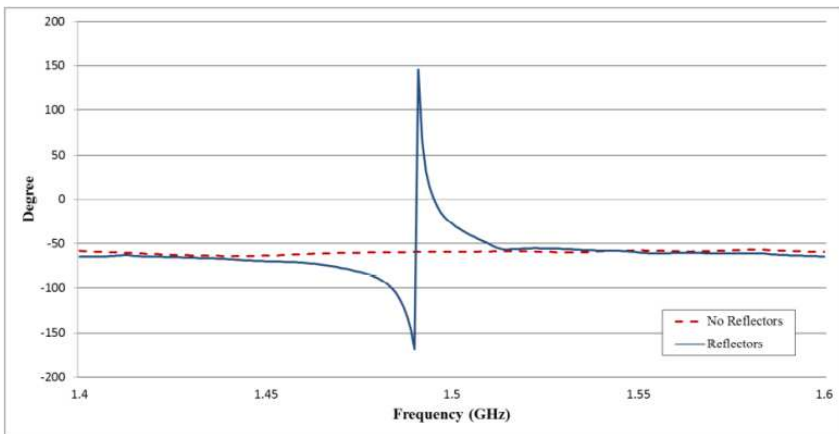


Figure 12. Measured phase vs. frequency with and without reflectors.

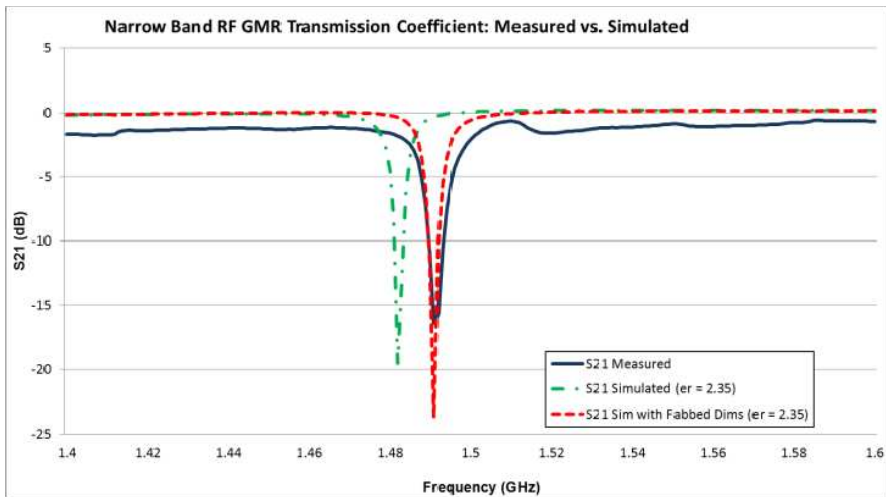


Figure 13. Measured transmission response along with simulated responses.

3 dB bandwidth of roughly 7 MHz. The measured device exhibited a 3 dB bandwidth of roughly 12 MHz.

The parameter w had essentially no effect on the operation of the GMR because diffraction occurs in the direction perpendicular to the grating grooves. It was chosen so the device would be approximately square and to prevent diffraction around the device edges from affecting the measurements.

7. CONCLUSION

Guided-mode resonance filters are an attractive alternative to metallic frequency selective surfaces when metals become problematic. They can provide a strong frequency response using just a simple dielectric structure. Typical GMR filters, however, are required to be hundreds of wavelengths long to operate, but this is not practical at radio frequencies where the wavelength can be large. This paper described a technique where a seven period GMR filter was designed and tested and the performance approached that of the infinitely periodic device. The technique involved incorporating spacer regions and reflective terminations on the ends of the device. Future work will focus on developing techniques to form the reflective terminations without using metals.

REFERENCES

1. Marconi, G. and C. S. Franklin, "Reflector for use in wireless telegraphy and telephony," US Patent 1,301,473, April 1919.
2. Munk, B. A., R. G. Kouyoumjian, and L. Peters, "Reflection properties of periodic surfaces of loaded dipoles," *IEEE Trans. on Ant. and Prop.*, Vol. 19, No. 5, 612–617, 1971.
3. Munk, B., *Frequency Selective Surfaces: Theory and Design*, Wiley, New York, 2005.
4. Marouby, E., J. R. Levrel, B. Bougerolles, J. Lenormand, and C. Terret, "On the use of frequency selective surfaces in stealth techniques for aerospace applications," *24th European Microwave Conference*, Vol. 1, 585–589, 1994.
5. Genovesi, S. and A. Monorchio, "Low profile array with reduced radar cross section," *IEEE URSI International Symposium on Electromagnetic Theory*, 799–802, 2010.
6. Lee, S.-W., "Scattering by dielectric-loaded screen," *IEEE Trans. on Ant. and Prop.*, Vol. 19, No. 5, 656–665, 1971.
7. Pelton, E. L. and B. A. Munk, "A streamlined metallic radome," *IEEE Trans. on Ant. and Prop.*, Vol. 22, No. 6, 799–803, 1974.
8. Raynes, D. L. and J. Delap, "Design of finite array with radome incorporating a frequency selective surface," *IEEE 2nd European Conference on Antennas and Propagation*, 1–5, 2007.
9. Agahi, S. and R. Mittra, "Design of a cascaded frequency selective surface as a dichroic subreflector," *Antennas and Propagation Society International Symposium*, 88–91, 1990.
10. Pozar, D. M., "Flat lens antenna concept using aperture coupled microstrip patches," *Electronics Letters*, Vol. 32, No. 23, 2109–2111, 1996.
11. Jalaly, I. and I. D. Robertson, "RF barcodes using multiple frequency bands," *IEEE MTT-S International Microwave Symposium Digest*, 139–142, 2005.
12. Wang, L. B., K. Y. See, J. W. Zhang, A. C. W. Lu, and S. T. Ng, "Full-wave modeling and analysis of screen printed EMI shield," *IEEE Asia-Pacific Microwave Conference Proceedings (APMC)*, 1348–1351, 2010.
13. Pugh, S., "Using FSS in HPM applications," MS Thesis, Air Force Institute of Technology, 2010.
14. Magnusson, R. and S. S. Wang, "New principle for optical filters," *Appl. Phys. Lett.*, Vol. 61, No. 9, 1022–1024, 1992.
15. Tibuleac, S. and R. Magnusson, "Reflection and transmission

- guided-mode resonance filters,” *J. Opt. Soc. Am A*, Vol. 14, No. 7, 1617–1626, 1997.
16. Boonruang, S., A. Greenwell, and M. G. Moharam, “Multiline two-dimensional guided-mode resonant filters,” *Appl. Opt.*, Vol. 45, No. 22, 5740–5747, 2006.
 17. Boyce, R. R. and R. K. Kostuk, “Investigation of the effect of finite grating size on the performance of guided-mode resonance filters,” *Appl. Opt.*, Vol. 39, No. 21, 3649–3653, 2000.
 18. Magnusson, R. and M. Shokooh-Saremi, “Physical basis for wideband resonant reflectors,” *Opt. Express*, Vol. 16, No. 5, 3456–3462, 2008.
 19. Rayleigh, L., *Proc. R. Soc. Lond. A*, Vol. 79, 399–416, 1907.
 20. Rumpf, R. C., “Design and optimization of nano-optical elements by coupling fabrication to optical behavior,” 236, Ph.D. Thesis, University of Central Florida, 2006.
 21. Balanis, C., *Advanced Engineering Electromagnetics*, 323–325, Wiley, New York, 1989.
 22. Hao, J. and L. Zhou, “Electromagnetic wave scatterings by anisotropic metamaterials: Generalized 4×4 transfer-matrix method,” *Phys. Rev. B*, Vol. 77, 094201, 2008.
 23. Grann, E. B., M. G. Moharam, and D. A. Pommet, “Artificial uniaxial and biaxial dielectrics with use of two-dimensional subwavelength binary gratings,” *J. Opt. Soc. Am. A*, Vol. 11, No. 10, 2695–2703, 1994.
 24. Moharam, M. G., E. B. Grann, D. A. Pommet, and T. K. Gaylord, “Formulation for stable and efficient implementation of the rigorous coupled-wave analysis of binary gratings,” *J. Opt. Soc. Am. A*, Vol. 12, No. 5, 1068–1076, 1995.
 25. Magnusson, R. and S. S. Wang, “New principle for optical filters,” *Appl. Phys. Lett.*, Vol. 61, No. 9, 60–84, 1992.